Extended Abstracts of the 2012 International Conference on Solid State Devices and Materials, Kyoto, 2012, pp939-940

Discrete Energy Levels in Synthesized Au Nanoparticle by Chemically Assembled Single-Electron Transistors

Shinya Kano[1,2], Kosuke Maeda[1,2], Daisuke Tanaka[2,3], Toshiharu Teranishi[2,4], Luke W. Smith[5], Charles G. Smith[5], and Yutaka Majima[1,2,6]

[1] Materials and Structures Laboratory, Tokyo Institute of Technology, 4259 Nagatsuta-cho, Midori-ku, Yokohama 226-8503, Japan
Phone: +81-45-924-5376 E-mail: kano@nanoele.msl.titech.ac.jp
[2] CREST, Japan Science and Technology Agency, Yokohama 226-8503, Japan
[3]Graduate School of Pure and Applied Sciences, University of Tsukuba, Tsukuba 305-8571, Japan
[4]Institute of Chemical Research, Kyoto University, Uji 611-0011, Japan
[5]Cavendish Laboratory, University of Cambridge, JJ Thomson Avenue, Cambridge CB3 0HE, UK
[6] Department of Printed Electronics Engineering, Sunchon National University, Sunchon 540-742, Korea

1. Introduction

Qubit defined by quantum dots has been attracting much attention because of its application for solid-state quantum information processing[1,2]. Quantum dots for qubit are classified into two important different types, self-assemble quantum dots and electrostatically defined quantum dots[1]. Measurements of discrete energy level spectra have been demonstrated in both types of quantum dots: semiconductor quantum dot[3], carbon nanomaterial[4], and metallic nanoparticles (NPs)[5]. Considering controllability and stability of device characteristics, chemically synthesized Au NPs with self-assembled monolayer (SAM) are highly useful quantum dots[6, 7]. Discrete energy level of quantum dots are expected as a two-level system of qubit.

Here, we analyzed the discrete energy level spectra of synthesized Au NP by chemically assembled single-electron transistor (SET) in detail. Synthesized Au NPs are chemically assembled as Coulomb island of SET. Spatial structure of Au NPs and electrodes are determined from the stability diagram of SET. Discrete energy level spectra of single Au NP are observed at 300 mK and mean level spacing is discussed with the theoretical value. By applying magnetic field, we observe the magnetic field evolution of discrete energy level spectra in Au NP.

2. Methods

The core diameter and standard deviation of synthesized Au NPs in SETs were 6.2 ± 0.8 nm. These Au NPs were protected by decanethiol molecules to stabilize every Au NPs. Stable SETs functionalized by SAM and Au NPs were simultaneously fabricated by the combination of the top-down and chemical bottom-up techniques[6, 7]. Initial structure of source, drain and two side-gate electrodes of Ti(2 nm)/Au(10 nm) was fabricated on a SiO_2(300 nm)/Si substrate by electron beam lithography (EBL), where the gap separation was approximately 25 nm. Nanogap electrodes were electroless-gold plated as previously reported methods and the gap separation can be controlled which is suitable for the size of Au NPs simultaneously[8]. After fabrication of the electroless-gold plated nanogap electrodes, the substrate was immersed in a 1 mM ethanolic solution of octanethiol for 24 h to form as SAMs. The substrate was then immersed in a 500 mM ethanolic solution of decanedithiol for 24 h. Finally, the substrate was immersed in a toluene solution of Au NPs for 12 h. Au NPs were self-assembled onto Au electrode surface selectively-anchored by decanedithiol molecules[6, 7]. These SET fabrication methods enable us to prepare multiple chemically assembled SET at the same time compared with other fabrication methods[5]. Fabricated device characteristics were measured at 300 mK. Drain current – drain voltage (I_d – V_d) characteristics and drain current – gate voltage (I_d – V_g) characteristics of SETs were measured by using voltage source, digital multimeter and preamplifier. The differential conductance of drain current – drain voltage (dI_d/dV_d – V_d) were calculated by numerical differentiating the I_d – V_d curve directly without lock-in amplifiers.

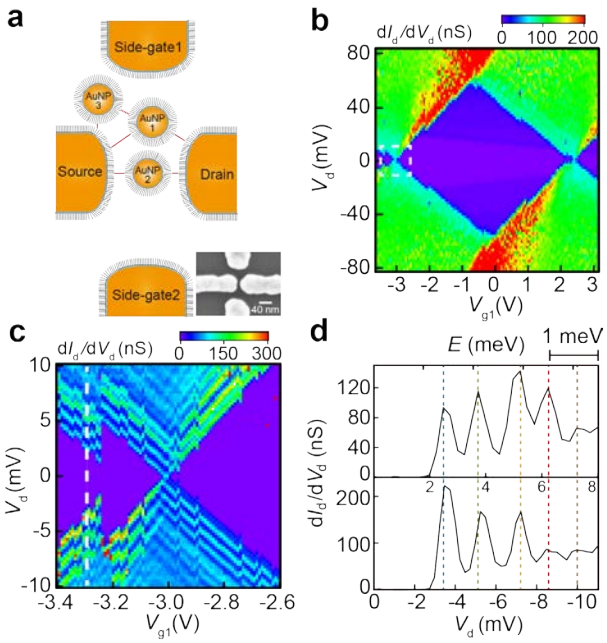

Fig.1 **a,** Schematic structure of fabricated chemically assembled SETs. SEM image of typical electroless-gold plated electrodes is shown below. **b,** Stability diagram of fabricated SET at 300 mK. White broken area indicates the region of Fig.1c. **c,** Stability diagram at degeneracy point of two Coulomb diamonds. White lines indicate the region of Fig.1d. **d,** dI_d/dV_d – V_d characteristics at V_{g1} = −3.3 V.

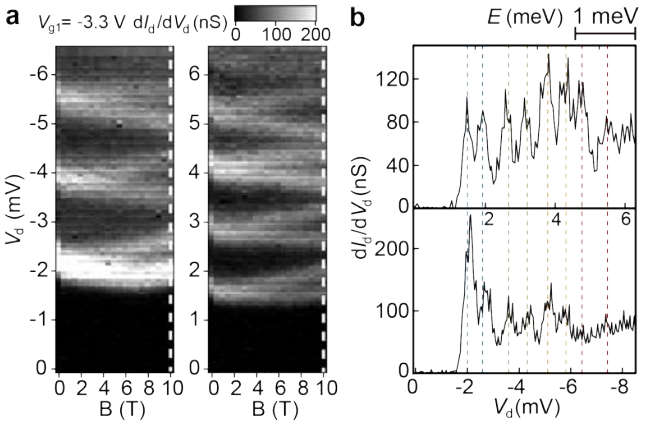

Fig.2 **a,** Magnetic field evolution of $dI_d/dV_d - V_d$ characteristics at $V_{g1} = -3.3$ V. White lines indicate the region of Fig. 2b. **b,** $dI_d/dV_d - V_d$ characteristics under B=10 T

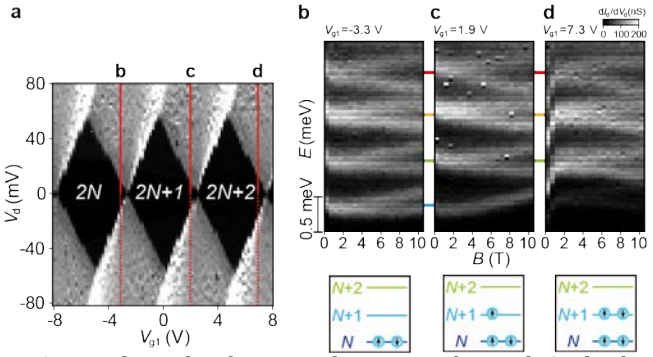

Fig.3 **a,** Relationship between electron number and Coulomb diamonds. N represents the number of energy level in Au NP. Solid lines are represented as Fig. 3b-d. **b-d,** Magnetic field evolution of dI_d/dV_d peaks at $V_{g1} = -3.3$ V (b), $V_{g1} = 1.9$ V (c), and 7.3 V (d) in positive V_d region. Electron configuration in excited energy levels of Au NP is shown below.

3. Results and Discussion

Figure 1a shows a schematic structure of chemically assembled SET consisting of Au NPs and nanogap electrodes. The number of Au NPs and their position in nanogap electrodes are determined from the stability diagram of the SET. Figure 1b shows a stability diagram obtained by differential conductance (dI_d/dV_d) of the SET as a function of side-gate1 voltage (V_{g1}) and V_d. Because two Au NPs (Au NP1 and Au NP2) are not capacitively coupled each other and work as a Coulomb island individually, two distinct rhombic-shaped Coulomb diamond are superimposed in the stability diagram. Au NP3 in Fig.1a works as a single-electron box and the SET can detect the electron transport of Au NP3 in the stability diagram. Figure 1c shows a stability diagram at the degeneracy points of two Coulomb diamonds and Fig. 1d shows $dI_d/dV_d - V_d$ characteristics at $V_{g1} = -3.3$ V. Every dI_d/dV_d peaks are originated from the discrete energy level of Au NP. The mean level spacing of Au NP is estimated as $\Delta E = 0.73$ meV considering a capacitive division of voltage across the two tunneling junction, which is consistent with the theoretical value using eq. (1),

$$\Delta E \approx \frac{2\pi^2\hbar^2}{m_e k_F V} , \qquad (1)$$

where m_e is the electron mass, k_F is the Fermi wave vector, and V is the volume of Au NP.

Figure 2a shows a magnetic field evolution of $dI_d/dV_d - V_d$ characteristics at $V_{g1} = -3.3$ V and Figure 2b shows $dI_d/dV_d - V_d$ characteristics under 10 T. Every dI_d/dV_d evolution reflect the split of excited energy states in Au NP by Zeeman effect. The g-factor of synthesized Au NP is 0.57, which agrees with previous report[5].

Figure 3a shows a relationship between the electron number and stability diagram. N is the Nth energy level in Au NP. Figures 3b-d show a magnetic field evolution of $dI_d/dV_d - V_d$ characteristics at each Coulomb diamond. The lowest excited energy states disappear as the electron number increases, which corresponds to the phenomena that electron transports into the lowest excited energy states as V_g increases.

4. Conclusion

In conclusion, we analyzed the discrete energy level spectra of synthesized Au NP by chemically assembled SET in detail. Chemically assembled SET show ideal Coulomb diamond and dI_d/dV_d peaks originated from excited energy level of Au NP. Magnetic field evolution of discrete energy level spectra shows Zeeman effect and the dependence on the electron number in Au NP. These results indicate that chemically assembled qubit can be one of the candidates for solid-state quantum information processes.

Acknowledgements

This study was partially supported by a Grant-in-Aid for Scientific Research on Innovative Areas (No. 20108011, π-Space) from the Ministry of Education, Culture, Sports, Science and Technology (MEXT); by a Grant-in-Aid for Scientific Research (A) (23245028) from MEXT (T.T.); by a Grant-in-Aid for Japan Society for the Promotion of Science (JSPS) Fellows from MEXT (S.K.); by the Collaborative Research Project of Materials and Structures Laboratory, Tokyo Institute of Technology; and by the World Class University (WCU) Program through the Ministry of Education, Science and Technology of Korea (R31-10022).

References

[1] T. D. Ladd, F. Jelezko, R. Laflamme, Y. Nakamura, C. Monroe, and J. L. O'Brien, Nature **464** (2010) 45-53.

[2] D. Loss and D. P. DiVincenzo, Phys. Rev. A **57** (1998) 120-126.

[3] D. R. Stewart, D. Sprinzak, C. M. Marcus, C. I. Durüoz, and J. S. Harris Jr., Science **278** (1997) 1784-1788.

[4] D. H. Cobden, M. Bockrath, P. L. McEuen, A. G. Rinzler, and R. E. Smalley, Phys. Rev. Lett. **81** (1998) 681-684.

[5] F. Kuemmeth, K. I. Bolotin, S.-F. Shi, and D. C. Ralph, Nano Lett. **8** (2008) 4506-4512.

[6] N. Okabayashi, K. Maeda, T. Muraki, D. Tanaka, M. Sakamoto, T. Teranishi, and Y. Majima, Appl. Phys. Lett. **100** (2012) 033101.

[7] K. Maeda, N. Okabayashi, S. Kano, S. Takeshita, D. Tanaka, M. Sakamoto, T. Teranishi, and Y. Majima, ACS Nano **6** (2012) 2798-2803.

[8] Y. Yasutake, K. Kono, M. Kanehara, T. Teranishi, M. R. Buitelaar, C. G. Smith, and Y. Majima, Appl. Phys. Lett. **91** (2007) 203107.